NOTICE: This is the accepted author manuscript of the publication

Early upregulation of 18-kDa translocator protein in response to acute neurodegenerative damage in TREM2-deficient mice

Sara Belloli[a, b, c], Maria Pannese[d], Cecilia Buonsanti[e], Chiara Maiorino[e], Giuseppe Di Grigoli[a, b], Assunta Carpinelli[a], Cristina Monterisi[f], Rosa Maria Moresco[b, c, f], Paola Panina-Bordignon[d]

a Institute of Bioimages and Molecular Physiology, National Research Council, Segrate, MI, Italy
b Milan Center for Neuroscience (NeuroMi), Milan, Italy
c Experimental Imaging Center, IRCCS San Raffaele Scientific Institute, Milan, Italy
d Division of Genetics and Cell Biology, IRCCS San Raffaele Scientific Institute, Milan, Italy
e Division of Neuroscience, IRCCS San Raffaele Scientific Institute, Milan, Italy
f Department of Medicine and Surgery, University of Milan Bicocca, Monza, Italy

Published in Neurobiology of Aging, available online 17 January 2017.

Doi: 10.1016/j.neurobiolaging.2017.01.010

Direct link to the final version of the article:

http://www.sciencedirect.com/science/article/pii/S0197458017300180

A CC-BY-NC-ND license apply to this work.

*Manuscript
Click here to view linked References

Early up-regulation of 18 kDa Translocator Protein in response to acute neurodegenerative damage in TREM2 deficient mice

Sara Belloli[a,b,f], Maria Pannese[c], Cecilia Buonsanti[d,1], Chiara Maiorino[d,2], Giuseppe Di Grigoli[a,b], Assunta Carpinelli[a], Cristina Monterisi[e], Rosa Maria Moresco[b,e,f] and Paola Panina-Bordignon[c].

[a] IBFM-CNR, Via Fratelli Cervi 93, 20090, Segrate (MI), Italy;
[b] Milan Center for Neuroscience (NeuroMi), Milan, Italy;
[c] Division of Genetics and Cell Biology, IRCCS San Raffaele Scientific Institute, Via Olgettina 58, 20132 Milan, Italy;
[d] Division of Neuroscience, IRCCS San Raffaele Scientific Institute, Via Olgettina 58, 20132 Milan, Italy;
[e] Department of Medicine and Surgery, University of Milan Bicocca, Via Cadore 48, 20900 Monza;
[f] Experimental Imaging Center, IRCCS San Raffaele Scientific Institute, Via Olgettina 58, 20132 Milan, Italy.

[1]C.B. current address: Novartis Vaccine and Diagnostics, Immunology, Via Fiorentina 1, 53100 Siena, Italy. [2]C.M. current address: Ufficio Valorizzazione Ricerche, Scuola Superiore Sant'Anna, P.zza Martiri della Libertà, 56127 Pisa.

R.M.M. and P.P.-B. equally contributed to study design and discussion.

Running Title: TREM2 role in acute neurodegeneration

Corresponding author:
Prof. Rosa Maria Moresco,
University of Milan Bicocca,
Via Fratelli Cervi 93, 20090 Segrate (MI), Italy
Phone: +39 0226433817
Fax : +39 0226432717;
Email: moresco.rosamaria@hsr.it

ABSTRACT

Mutations in the TREM2 gene confer risk for Alzheimer and susceptibility for Parkinson Disease (PD). We evaluated the effect of TREM2 deletion in a MPTP-induced PD mouse model, measuring neurodegeneration and microglia activation using a combined *in vivo* imaging and *post mortem* molecular approach.

In wild type (wt) mice, MPTP administration induced a progressive decrease of [^{11}C]FECIT uptake, culminating at day 7. Neuronal loss was accompanied by an increase of TREM2, IL-1β, and TSPO transcript levels, [^{11}C]PK11195 binding and GFAP staining (from day 2), and an early and transient increase of TNF-α, Galectin-3 and Iba-1 (from day 1). In TREM2 null (TREM2$^{-/-}$) mice, MPTP similarly affected neuron viability and microglial cells, as shown by the lower level of Iba-1 staining in basal condition, and reduced increment of Iba-1, TNF-α, IL-1β in response to MPTP. Likely to compensate for TREM2 absence, TREM2$^{-/-}$ mice showed an earlier increment of [^{11}C]PK11195 binding and a significant increase of IL-4. Taken together, our data demonstrate a central role of TREM2 in the regulation of microglia response to acute neurotoxic insults, and suggest a potential modulatory role of TSPO in response to immune system deficit.

Keywords: Triggering receptor expressed on myeloid cells 2, Parkinson Disease, neuroinflammation, 18 kDa Translocator Protein, Positron Emission Tomography

1. INTRODUCTION

Triggering receptor expressed on myeloid cells 2 (TREM2) is a membrane spanning receptor belonging to the immunoglobulin and lectin-like superfamily (Bouchon, et al., 2001). TREM2 binds to still unknown ligands and induces association with the immunoreceptor tyrosine–based activation motif (ITAM) containing adaptor protein DAP12. The association is followed by recruitment of multiple stimulatory effectors, including kinases (ZAP70, SYK, PI3K), and phospholipase Cγ. Once assembled, the ITAM-based transduction complex delivers activation signals to the cell, e.g. myeloid cells, including dendritic cells, which regulate T cell responses and microglia activation. The complex of TREM2 and its adaptor protein DAP12 is expressed by microglia in both human and mouse CNS (Piccio, et al., 2008, Schmid, et al., 2002). Although its expression has been reported also on the cell surface, the bulk of TREM2 is stored in intracellular pools that can be rapidly translocated to the cell surface (Sessa, et al., 2004).

Under physiological conditions, microglia cells are quiescent and distributed throughout the central nervous system (CNS). In response to a variety of stimuli such as axonal injury, ischemia, trauma and neurodegenerative diseases, microglia cells become rapidly activated Perry, 2010). Whether microglia activation is beneficial or detrimental is still under debate and may depend on both the environment and the nature of the stimulus (Polazzi and Monti, 2010). Several observations indicate that activation of microglia is involved in the progression of different neuroinflammatory or neurodegenerative disorders such as multiple sclerosis (Lassmann, 2007), amyotrophic lateral sclerosis (Henkel, et al., 2009), AIDS dementia complex (Yadav and Collman, 2009), prion disease (Minghetti and Pocchiari, 2007), Alzheimer's disease (Naert and Rivest, 2011) and Parkinson's disease (PD) (Long-Smith, et al., 2009) through the release of a variety of proinflammatory and potentially neurotoxic substances (Perry, 2010). Nevertheless, activated microglia seems to exert also

beneficial functions such as the secretion of neurotrophins (Bessis, et al., 2007), the removal of tissue debris (Napoli and Neumann, 2010), and the promotion of axonal growth (Hynds, et al., 2004). It remains uncertain, however, what triggers activation of microglia in different disorders and if the activated form can be targeted to influence the natural prognosis.

Several recent observations underline the role of TREM2 in the protective function of microglial cells (Painter, et al., 2015,Wang, et al., 2016). Firstly, TREM2 over-expression in microglia induces cytoskeleton reorganization, augments phagocytosis, and modulates TNF-α, IL-1β and NOS-2 production, suggesting that TREM2 may exert anti-inflammatory functions (Takahashi, et al., 2005). Secondly, TREM2-transduced myeloid cells, intravenously injected, ameliorate experimental autoimmune encephalomyelitis (EAE), a mouse model of multiple sclerosis, by migrating into the inflammatory lesions in the spinal cord, promoting lysosomal and phagocytic activity, clearing degenerated myelin, and creating an anti-inflammatory cytokine milieu within the CNS (Takahashi, et al., 2007). Finally, we have demonstrated that TREM2 is highly expressed in the CNS microglia during EAE, and that blockade of TREM2 in the active phase of EAE results in disease exacerbation with more diffuse CNS inflammatory infiltrates and demyelination in the brain parenchyma (Fenoglio, et al., 2007, Piccio, et al., 2007). Based on these data, we suggested that TREM2 expression on microglial cells correlates with a specific activated phenotype that exerts important protective functions such as phagocytosis of dying cell, control of local inflammation, and promotion of tissue repair.

A direct link between TREM2 dysfunction and neurodegeneration emerged from the studies in patients with Nasu-Hakola disease (NHD; polycystic lipomembranous osteodysplasia with sclerosing leukoencephalopathy). NHD is a rare autosomal recessive disorder clinically characterized by presenile frontal-type dementia and systemic bone cysts, associated with loss-of-function mutations in TREM2 and DAP12 (Numasawa, et al., 2011,Paloneva, et al.,

2002). The brain pathology observed in NHD patients suggests that disruption of the TREM2/DAP12 pathway leads to neurodegeneration with a major and early involvement of the white matter, including loss of myelin and axons. Furthermore, a rare missense mutation (rs75932628, p.R47H) in the TREM2 gene represents an important risk factor for Alzheimer's disease (AD) (Finelli, et al., 2015) as well as other neurodegenerative disorders like fronto-temporal dementia and Parkinson's disease (Rayaprolu, et al., 2013). On the other hand, deletion of TREM2 gene exacerbates neurodegeneration in different animal models of AD (Wes, et al., 2016).

Another emerging regulatory target for microglial functions is represented by the 18 kDa Translocator Protein (TSPO) previously known as peripheral benzodiazepine receptor. TSPO is only minimally expressed in normal brain parenchyma but its levels rise upon microglia activation or macrophage infiltration (Winkeler, et al., 2012). These two events can be extensively visualized in different neurodegenerative, infective or inflammatory disorders using Positron Emission Tomography (Rayaprolu, et al.) and radiopharmaceuticals that target TSPO. Although TSPO functional role is still under evaluation, it has been shown that TSPO-specific ligands exert protective effects against neurotoxic or neuroinflammatory insults (Choi, et al., 2011, Veiga, et al., 2007).

To evaluate if TREM2 expression could represent a marker of neuronal loss and/or microglial function in neurodegenerative processes, we analyzed a mouse model of PD induced by the administration of the neurotoxin 1-methyl 4-phenyl 1,2,3,6-tetrahydropyridine (MPTP) into wild type and TREM2 null mice (TREM2$^{-/-}$). In these mice, we evaluated by Positron Emission Tomography (PET) imaging the loss of nigrostriatal dopaminergic neurons using the radiotracers [^{11}C]FE-CIT and the activation of the microglia using the TSPO ligand [^{11}C]PK11195, and the inflammatory state by measuring glial markers and the release of proinflammatory cytokines.

2. MATERIALS AND METHODS

2.1 Animals and MPTP-treatment

TREM2$^{-/-}$ mice were generated as described (Turnbull, et al., 2006). TREM2$^{-/-}$ mice and C57BL/6 control littermates (8-12 weeks of age) received 4 intra-peritoneal (i.p.) injections at 2 hours intervals of either vehicle (PBS) or MPTP-HCl (20 mg/kg of free base in PBS; Sigma-Aldrich, Italy). This dose was chosen as it has been shown to be the lowest producing significant loss of striatal dopamine and dopamine active transporter (DAT) levels with a concomitant increase in striatal and nigral activated microglia expressing TSPO (Jackson-Lewis and Przedborski, 2007). MPTP handling and safety measures were in accordance with published guidelines. Radiopharmaceuticals used for *ex vivo* and *in vivo* studies were prepared in our facility as described below. Animal experiments were carried out in compliance with the institutional guidelines for the care and use of experimental animals (IACUC), which have been notified to the Italian Ministry of Health and approved by the Ethics Committee of the San Raffaele Scientific Institute.

2.2 Real Time PCR

One, two or seven days after MPTP intoxication, seven mice per group per time point were sacrificed, and the striatum, cerebellum and pons were dissected from the brains. An area corresponding to the ventral midbrain containing the substantia nigra (SN) was also isolated. Total RNA was extracted from tissue samples with Trizol Reagent (Invitrogen) according to the manufacturer's recommendations. After digestion with Dnase RNase-free (Promega) for 30 minutes at 37°C, RNA was purified by using RNeasy Mini kit (Qiagen). The cDNA synthesis was performed by using the ThermoScript RT-PCR System (Invitrogen, Italy) and Random Hexamer (Invitrogen), according to the manufacturer's instructions in a final volume of 20 µl. Quantitative real-time PCR analysis was performed using LightCycler 480

SYBR Green I Master Mix (Roche) on the LightCycler 480 Instrument (Roche) according to the manufacturer's PCR parameters. All analyses were performed in triplicate and the relative amount of the targets were normalized with the housekeeping gene β-actin. The $2^{-\Delta\Delta CT}$ method was used to calculate the relative changes in gene expression and expressed as fold change (F.C.) ± SD.

For the first set of qRT-PCR experiments, mouse TREM-2, β-actin (4352341E)VIC, Galectin-3 (Mm00802901_m1)FAM and TNFα (Mm 00443258)FAM primers were purchased from Applied Biosystems Italy and used at the recommended dilutions.

For the second set of qRT-PCR experiments, the following specific mouse primers (Sigma Aldrich) were used:

β-actin: FW: 5' gactcctatgtgggtgacgagg 3'; RV: 5' catggctggggtgttgaaggtc 3';

Trem2: FW: 5' gcacctccaggaatcaagag 3'; RV: 5' gggtccagtgaggatctgaa;

Tspo: FW: 5' tcagcggctaccaacct 3'; RV: 5' caggattcaggcatggtgat 3';

Il-1β: FW: 5' gcccatcctctgtgactcat 3'; RV: 5' aggccacaggtattttgtcg 3';

Il-4: FW: 5' tcaacccccagctagttgtc 3'; RV: 5' tgttcttcgttgctgtgagg 3'.

2.3 Immunofluorescence microscopy

In order to estimate microglia activation and reactive gliosis, the expression of ionized calcium binding adaptor molecule 1 (Iba-1) and of glial fibrillary acidic protein (GFAP) antigens were evaluated in the brain of $TREM2^{-/-}$ (day 1) or wt (day 1, 2 and 7) mice treated with PBS (n=3) or MPTP (n=3). Antibodies specific for GFAP and Iba-1 were purchased by Novus Biologicals (Italy) or Abnova (Germany). Mice were perfused with PBS followed by 4% paraformaldehyde (PFA). Brains were removed, post-fixed in PFA 4% for 16 hrs and sectioned on a cryostat as 10 µm thick sections after overnight cryo-protection in 20% sucrose. Sections were permeabilized with 0.1% Triton X-100 for 5 minutes and, after blocking with 10% FCS plus 1% BSA in PBS for 1h, incubated for 1h at RT with primary

Iba-1 and GFAP antibodies diluted respectively 1:500 and 1:1000 in PBS and secondary antibody Alexa fluor 488 (Abcam, UK) diluted 1:500 in PBS. Sections were then visualized using Confocal Laser Microscope Leica TCS SP8 (Leica Microsystems, Germany). Confocal images were analyzed counting three fields for each animal (n=3) and positive cells quantified using InForm software version 2.0 (PerkinElmer, Waltham, MA) and expressed as % of positive cells on total counted.

2.4 Radiopharmaceuticals in *ex vivo* and *in vivo* studies

The integrity of nigrostriatal dopaminergic neurons was evaluated *ex vivo* and *in vivo* using the dopamine transporters radioligand [^{11}C]*N*-2-fluoroethyl-2-β-carbomethoxy-3-β-(4-iodophenyl)-nortropane ([^{11}C]FECIT). [^{11}C]FECIT as well as other tropane derivatives, have been widely used for the evaluation of nigrostriatal neurons integrity, not only in patients with extrapyramidal disorders but also in preclinical model of PD (Halldin, et al., 1996,Lucignani, et al., 2002). Microglia activation was evaluated using the ^{11}C-labelled isoquinolinecarboxamide PK11195 ([^{11}C]PK11195) a ligand that binds to the 18 kDa Translocator Protein (TSPO) allowing the in vivo Positron Emission Tomography (Banati, et al., 2000).

2.5 MPTP effect on [^{11}C]PK11195 to TSPO: time course in WT mice.

A large number of studies have shown that TSPO levels are strongly increased following brain injury, in association with activation of microglial cells (Casellas, et al., 2002). The use of PET with the TSPO ligand [^{11}C]PK11195 have been extensively applied for the *in vivo* monitoring of microglia activation in brain diseases (Turkheimer, et al., 2015). To measure microglia activation using emission tomography techniques, on days 1, 2 and 7 after MPTP intoxication or PBS administration, C57BL/6 mice (n= 5 on day 1 and 2 and n= 7 on day 7) were injected in the tail vein with 73.3±24.2 μCi of [^{11}C]PK11195 (Specific Activity=1.4±1.0 Ci/μmol at the time of injection). One hour after the tracer injection,

205 animals were sacrificed and brain areas (striatum and cerebellum) rapidly collected and
206 placed in pre-weighed tubes for gamma-counter counting. After decay correction,
207 radioactivity concentration was calculated as percentage of the injected dose per gram of
208 tissue (%ID/g).

209 **2.6 MPTP effect on [^{11}C]PK11195 to TSPO: TREM2$^{-/-}$ versus wt mice**

210 One day after MPTP-treatment, TREM2$^{-/-}$ and C57BL/6 mice (four animals per group), and
211 PBS-treated TREM2$^{-/-}$ and C57BL/6 mice, were injected in the tail vein with 119.3±32.8
212 μCi of the radioligand [^{11}C]PK11195 (Specific Activity = 9.0 Ci/μmol at the time of
213 production). One hour after tracer injection, animals were sacrificed and blood and brains
214 were processed as mentioned above for the radioactivity concentration determination.
215 Binding of [^{11}C]PK11195 to peripheral benzodiazepine receptors is usually calculated as a
216 ratio between target tissue (*i.e.*, TSPO expressing tissue) and a reference region that, in the
217 case of TSPOs studies, is represented by normal brain parenchyma. However, since it is not
218 possible to define *a priori*, among the different sampled brain areas, a region that is surely
219 devoid of activated microglia, radioactivity concentration (%ID/g) was used to define ligand
220 binding and to compare the different groups of animals and conditions as for *ex vivo*
221 experiments.

222 **2.7 MPTP effect on DAT: time course in wild-type mice**

223 *Ex vivo* binding of [^{11}C]FECIT was evaluated on day 1, 2 and 7 after MPTP intoxication or
224 PBS administration in C57BL/6 mice. Animals (n=5 for each time point or treatment group)
225 were injected in the tail vein with 73±29.2 μCi of the radioligand [^{11}C]FECIT (Specific
226 Activity= 1.4±0.2 Ci/μmol at the time of injection) and one hour later, sacrificed under gas
227 anesthesia. Brains were rapidly removed and the striatum and cerebellum collected and
228 placed in heparinized pre-weighted tubes for gamma-counting (LKB Compugamma CS
229 1282). After decay correction, radioactivity concentration was calculated as percentage of

the injected dose per gram of tissue (%ID/g). DAT availability was calculated as target region to cerebellum radioactivity concentration ratio. The cerebellum was used as reference region for the estimation of free, non-displaceable fraction of radioactivity since it contains negligible amounts of DAT (Laakso, et al., 1998).

2.8 MPTP effect on DAT: TREM2$^{-/-}$versus wild-type mice

For *ex vivo* studies, MPTP (n=21) or PBS (n=16) injected TREM2$^{-/-}$ mice, and MPTP (n=8) or PBS (n=8) injected wt mice, were injected in the tail vein with 64.1±29.3 μCi of [^{11}C]FECIT (Specific Activity= 2.2±1.6 Ci/μmol at the time of injection), seven days after MPTP intoxication. One hour after the injection, animals were sacrificed and processed as described above. The brain was divided in the two hemispheres: the left part was processed for the immunohistochemistry or RT-PCR while the right part was dissected in frontal cortex, striatum and cerebellum. Brain regions and a blood sample were placed in pre-weighed tubes and counted in a gamma-counter. Radioactivity concentration and DAT availability were calculated as indicated above.

Twelve additional animals (three for each group, *i.e.*, TREM2$^{-/-}$ or wt, and treatment, *i.e.*, PBS or MPTP group) were evaluated *in vivo* with [^{11}C]FECIT using a dedicated tomograph (YAP-(S)PET II, ISE S.r.l., Italy). Mice were anesthetized with 1.7% tribromoethanol solution (10 μl/g of weight, *i.p.*) and positioned supine on the animal PET bed, with the brain centered in the field of view (FOV). The acquisition started 45 min after the injection of 84.2±35.7 μCi of the radioligand [^{11}C]FECIT and lasted 30 min (mean acquisition time 60 min post injection). Brain radioactivity concentration was acquired in list mode using the full axial acceptance angle of the scanner (3D mode) and then reconstructed with the Expectation Maximization (EM) algorithm (Motta, et al., 2005). After correction for the isotope half-life and calibration with a dedicated phantom, PET images were co-registered with 3D-volumetric T2-weighted MRI sequences (Achieva 3T with mouse coil, Philips

Medical Systems, The Netherlands) obtained for the same animals on a day close to PET acquisition, using PMOD 2.7 software. Circular ROIs for striatum (area= 5.9 mm^2) and cerebellum (area= 6.7 mm^2) were identified on co-registered images and associated radioactivity was expressed as %ID/g. DAT availability was calculated as indicated for the *ex vivo* experiments.

2.9 Statistical analysis

Statistical evaluation of RT-PCR data was carried out by ONE-way ANOVA test or Student's t test with Mann Whitney's correction. Statistical evaluations of [^{11}C]FECIT and [^{11}C]PK1195 uptakes were carried out by ONE-way ANOVA test with Dunnett's correction. Analyses were performed using the Prism V5.0 software (Graph-Pad, San Diego, CA, USA). Statistical significance was accepted when * $p<0,05$, ** $p<0.01$ and *** $p<0.001$.

3. RESULTS

3.1 TREM2 transcripts are differentially modulated in different brain regions after MPTP treatment.

In order to investigate the role of TREM2 in Parkinson's disease (PD), we used the MPTP mouse model of neurodegeneration. TREM2 expression was measured by RT-PCR in four different brain regions of MPTP and PBS-injcted mice on day 1, 2 and 7. In the substantia nigra (SN), the expression of TREM2 increased slowly reaching the highest level 7 days after MPTP treatment. In the striatum, MPTP-induced TREM2 up-regulation started on day 1 post-MPTP and reached the highest level on day 2 post-MPTP. In the cerebellum, TREM2 expression was up-regulated on day 1 after MPTP and then decreased to basal levels, while no significant increase of TREM2 expression was observed in the pons (Figure 1).

278 **3.2 Microglia displays an activated phenotype upon MPTP treatment.**

279 Once activated, microglia strongly upregulates Iba-1 and Gal-3 expression (Venkatesan, et
280 al., 2010). At day 1 after MPTP administration, Gal-3 expression was significantly increased
281 in both SN and striatum, and persisted in the latter until day 2 (Figure 2A). In addition, we
282 observed a marked increase of both Iba-1 and GFAP immunofluorescence in striatum of
283 MPTP-treated animals, although with a different kinetics (Figure 2B). Iba-1 fluorescence,
284 expressed as percentage of positive cells, was maximum on 1 day post-MPTP ($p<0,01$) and
285 remained significantly high ($p<0,05$) even on day 2 (Figure 2C). The presence of reactive
286 gliosis was confirmed by GFAP staining that was evident starting from day 2 (Figure 2B,
287 right). Moreover, the microglia in the striatum showed an activated hypertrophic phenotype
288 at the time of maximal Iba-1 expression (day 1) (Figure 2B), becoming ramified at later
289 time points (day 2 and day 7) (Figure 2 B).

290 Microglial activation was further evaluated by measuring binding of the TSPO radioligand
291 [^{11}C]PK11195 in those brain regions with the highest expression of TREM2 transcript (SN,
292 striatum) (Figure 3A). MPTP promoted an increase of radioligand uptake starting from day
293 2, which was significantly high in the striatum (76,7%, $p<0.01$) and that remained high
294 thereafter (65,3%, $p<0,01$). TSPO transcripts levels were determined in striatum to confirm
295 [^{11}C]PK11195 uptake data. Differently to Gal-3 and Iba-1 expression that rapidly reverted to
296 the basal level after MPTP treatment, TSPO mRNA in the striatum increased starting from
297 day 2 and remained high thereafter (Figure 3B), corroborating [^{11}C]PK11195 uptake results.
298 These results suggest that the kinetics of TSPO strongly correlates with the modulation of
299 TREM2 expression (Figure 1). Consistent with an ongoing inflammatory response, at early
300 times after MPTP, we observed a significant but transient increase in TNF-α mRNA
301 transcripts in the striatum and to a minor extent in the SN (Figure 3C), and a progressive

increase of IL-1β. MPTP induced also a slight and progressive increase of IL-4 that peaked at day 7 (Figure 3D).X

3.3 Lack of TREM2 affects microglia phenotype and modulates TSPO and TNF-α during MPTP injury.

To test if TREM2 is involved in the modulation of microglia activation in response to the neurotoxin insult, we evaluated microglia activation in TREM2$^{-/-}$ versus wt mice treated with MPTP. Immunofluorescence for Iba-1 showed that, only few faintly immunoreactive microglia cells were present in the striatum of wt and TREM2$^{-/-}$ PBS-injected mice. On day 1 after MPTP treatment, a significant increase of Iba-1 positive cells were observed in both wt ($p>0.001$) and TREM2$^{-/-}$ ($p<0.05$) mice (Figure 4A). Interestingly, in TREM2$^{-/-}$ mice, Iba-1 expression was significantly lower than in wt mice, both at baseline (PBS) and after MPTP treatment ($p<0.05$). On the contrary, basal levels of GFAP immunostaining were similar in wt and TREM2$^{-/-}$ animals, but a significant increase was observed only in wt mice at day 1 post-MPTP treatment. Figure 4B shows a representative immunofluorescence staining of Iba-1 and GFAP in striatum of wt and TREM2$^{-/-}$ mice after PBS injection or MPTP treatment (day 1).

Different results were obtained when TSPO expression was analyzed using [^{11}C]PK11195. On day 1 after MPTP treatment, TREM2$^{-/-}$ mice showed an earlier and stronger significant increase of radioligand uptake in comparison to wt mice, (see Figure 4C). [^{11}C]PK11195 binding was significantly increased in the striatum (129% increase, $p<0.01$) and in the SN (112% increase, $p<0.05$) of TREM2$^{-/-}$ mice at day 1 after MPTP in comparison to PBS injected mice, and this increase was paralleled by a reduction of TNF-α and IL-1β expression (Figure 5A, right and 5B). However, the increase in radioligand binding was not accompanied by an increase in TSPO transcript expression (Figure 4D). Moreover, RT-PCR analysis showed that at day 1 after intoxication the expression of Gal-3 in the striatum and

SN of TREM2$^{-/-}$ mice was comparable to that observed in wt animals (Figure 5A, left). Finally the basal expression of IL-4 was significantly higher ($p<0.05$) in TREM2$^{-/-}$ compared to wt animals (Figure 5B).

3.4 [^{11}C]FECIT studies reveal comparable levels of striatal DAT availability in MPTP-treated TREM2$^{-/-}$ and wt mice.

To evaluate the role of TREM2 on neuronal vulnerability, we compared the effect of MPTP administration on striatal dopamine transporter (DAT) expression in wt and TREM2$^{-/-}$ mice. In wt mice, DAT availability, expressed as striatum to cerebellum ratio of [^{11}C]FECIT uptake, was decreased by 43% at day 1 after MPTP administration (2.58 ± 0.48 in controls *vs* 1.47 ± 0.20 in MPTP-treated animals; p=0.001), and it reached the nadir at day 7 (49%; 1.32 ± 0.18; p=0.0004) (Figure 6A). [^{11}C]FECIT uptake remained stable until day 14 (see Supplementary Figure 1). As expected, [^{11}C]FECIT uptake in the cortex was not affected by MPTP treatment (see Supplementary Figure 2).

Similar levels of [^{11}C]FECIT uptake in the striatum were found in both wt and TREM2$^{-/-}$ mice injected with PBS or treated with MPTP (Figure 6B). [^{11}C]FECIT uptake ratios were 2.47 ± 0.13 and 2.28 ± 0.54 in PBS-injected wt and TREM2$^{-/-}$ mice, respectively. Seven days after MPTP treatment, these values were reduced to 1.38 ± 0.44 in wt (-44%; p< 0.0001) and to 1.34 ± 0.15 in TREM2$^{-/-}$ mice (-41%; p< 0.0001). Therefore, DAT activity loss in the striatum after MPTP treatment was not different in TREM2$^{-/-}$and wt mice.

These findings were confirmed by *in vivo* PET studies (Figure 6C). In PBS-injected mice, [^{11}C]FECIT uptake in striatum was 1.39 ± 0.39 in wt and 1.57 ± 0.11 in TREM2$^{-/-}$ mice (Figure 6C, I and III respectively), while in MPTP-treated mice, the uptake was reduced both in wt (1.16 ± 0.03; -21%; p= 0.01) and in TREM2$^{-/-}$ mice (24 ±0 .06; -17%; p= 0.1) (Figure 6C, II and IV respectively).

4. DISCUSSION

Although the link between microglia activation and dopaminergic neuronal death is well established (Block and Hong, 2007), the role of activated microglia in inflammatory processes and pathogenesis of Parkinson's disease (PD) is still under investigation (Long-Smith, et al., 2009, Perry, 2010, Sanchez-Guajardo, et al., 2015). Preclinical studies suggested that microglia activation might contribute to later degeneration of dopamine neurons starting from the substantia nigra (SN). Damaged neurons activate microglia to produce neurotoxic factors, which induce surrounding neurons in perpetuating toxicity. Therefore, the possibility to interfere with the inflammatory events that accompany neurodegeneration in PD might offer interesting therapeutic options. TREM2 expressed by microglia is known to modulate the inflammatory response by suppression of microglia-mediated cytokine production and secretion, and by regulation of phagocytic pathways that clear neuronal debris (Hsieh, et al., 2009, Van Der Putten, et al., 2012). The present study analyzes the possible correlation of TREM2 with the increased inflammatory state associated to the development of neurodegenerative diseases, such as PD, by modulating the activation state of microglia and possibly exerting a beneficial role. In order to investigate this aspect, we used an experimental animal model in which the death of the nigrostriatal dopaminergic neurons in the SN is induced by the neurotoxin MPTP (Smeyne and Jackson-Lewis, 2005). This mouse model recapitulates most of the pathological hallmarks of PD, including loss of dopamine content in the striatum and behavioral deficits.

We and others, have previously suggested that TREM2 expression on microglia and macrophages in the CNS correlates with a specific cell phenotype that exerts important protective functions in EAE and animal models of Alzheimer disease, brain ischemia and aging (Jay, et al., 2015, Kawabori, et al., 2015, Poliani, et al., 2015,). In humans, elevated

levels of soluble TREM2 were detected in cerebrospinal fluid of multiple sclerosis patients (Piccio, et al., 2008) and several loss of function mutations in the TREM2 gene are associated with neurodegenerative disorders like AD, FTD and PD (Finelli, et al., 2015, Rayaprolu, et al., 2013, Wes, et al., 2016). However, the precise role of microglia in neurodegenerative and neuroinflammatory disorders, and the modulatory effect exerted by TREM2 are still debated, although available results indicate that they may have different functions in different phases of the disease. In the PD model induced by MPTP, microglia activation is suggested to be driven by neuronal death (Bessis, et al., 2007).

Here we show that TREM2 transcripts are up-regulated primarily in the striatum and SN after MPTP treatment. Microglia activation is also observed in the same areas, as shown by increased TSPO ligand binding and transcript levels, and by a fast increase of Iba-1 and Gal-3 expression at day 1 post-MPTP. This was confirmed by immunofluorescence, where Iba-1 positive cells reached the maximum at this time point, corresponding also to the phagocytic amoeboid state. Indeed, upregulation of Iba-1 and Gal-3 expression follows activation of microglia after neuroinflammation or brain injury (Venkatesan, et al., 2010). As expected, increased levels of GFAP were observed only from day 2. It is known that astrocytes mediate the MPTP-dependent toxicity towards dopaminergic neurons through the production of the cytotoxic agent MPP^+ leading to an increase in GFAP expression, that occurs after dopaminergic neurons death in striatum and SN (Przedborski, et al., 2000).

$TREM2^{-/-}$ mice showed a lower pro-inflammatory response to MPTP as indicated by the mild increase in TNF-α and IL-1β compared to wt animals. In addition $TREM2^{-/-}$ mice presented lower levels of the microglial marker Iba-1 even in the absence of neurotoxic insults. In line with these findings, TSPO, another marker of an ongoing immune response in the brain (Casellas, et al., 2002) was differently displayed in absence of TREM2. Indeed, $TREM2^{-/-}$ mice showed an earlier and stronger response to the neurotoxin in terms of

401 [^{11}C]PK11195 binding in comparison to wt animals. On the contrary we failed to observe
402 any significant differences of GFAP levels in TREM2$^{-/-}$ mice compared to wt, confirming
403 the selectivity of TREM2 for microglia/monocyte cells.
404 The exact role of microglia and pro-inflammatory cytokines in the development of MPTP-
405 induced neuronal loss, as well as in other acute neuronal injury conditions, is still debated as
406 it has been reported to have both a neuroprotective and a lethal influence on neuronal
407 viability (Sieber, et al., 2013).
408 Takahashi et al. have shown that microglia with functionally impaired TREM2 expression
409 have increased gene transcription of inflammatory mediators when compared to apoptotic
410 neurons, suggesting that TREM2 deficiency causes dysregulation of microglial phagocytosis
411 and release of inflammatory mediators; these phenotypes are associated with an advanced
412 loss of cerebral axons and myelin, and the activation of microglia (Takahashi, et al., 2007,
413 Takahashi, et al., 2005, Wang, et al., 2015). Neuronal death induces microglia activation,
414 and the activated state *per se* could in turn cause dopaminergic neuronal death. Thus, to test
415 if the absence of TREM2 on microglia, and the associated impaired inflammatory
416 phenotype, could affect dopaminergic neuron survival after MPTP, we quantified the
417 amplitude of dopaminergic neuron mortality by following DAT expression. DAT is a
418 protein complex mostly expressed on pre-synaptical dopaminergic nerve terminal that is
419 reduced in the SN and striatum of patients with PD as well as of MPTP-induced PD mice
420 (Antonini, et al., 2002). DAT *in vivo* expression was evaluated with the specific radioligand
421 [^{11}C]FECIT, previously used to evaluate dopamine nerve terminal status in PD patients
422 (Antonini, et al., 2002). In the MPTP model, a progressive reduction of DAT levels was
423 observed in the striatum of wt mice, starting on day 1 after toxin treatment (45% reduction
424 of [^{11}C]FECIT uptake) and culminating at day 7 (54% reduction). TREM2$^{-/-}$ mice showed a

425 similar behavior. Taken together our results indicate that the reduced inflammatory reaction
426 observed in TREM2$^{-/-}$ mice does not protect against the MPTP induced neuronal injury.
427 In wt animals, microglia activation measured by TSPO ligand uptake occurred at day 2 after
428 intoxication and persisted until day 7 along with TREM2 overexpression in the striatum and
429 SN. On the contrary, dopaminergic neuron death almost reaches its maximum at day 1 after
430 intoxication, together with an increase of Iba-1, and TNF-α mRNA levels that were not
431 detectable at day 2 when the increase in [^{11}C]PK11195 binding and TREM2 expression was
432 maximum.
433 The different kinetics of neuronal cell death, microglia activation and TREM2 expression
434 suggest that TREM2 may play a prominent role in the regulation of the brain immune
435 system following to neuronal death rather than during the early phase of the acute
436 inflammatory phase triggered by microglia activation. On the other hand, results from our
437 and other studies suggest a major role of TREM2 in later events of acute neurological insults
438 or in chronic inflammatory diseases of the CNS rather than in acute neurological insults
439 phase, where an impairment of cell metabolism leads to simultaneous neuronal cell death
440 and microglia activation (Sieger and Peri, 2013).
441 Lack of TREM2 did not modify the total loss of dopaminergic neurons by apoptosis that
442 followed the acute administration of MPTP but rather promoted a higher and earlier
443 microglia activation as revealed by [^{11}C]PK11195 uptake studies and a lower release of pro-
444 inflammatory cytokines. Interestingly, the early increase in [^{11}C]PK11195 was not related to
445 modifications in TSPO mRNA levels, indicating a fast recruitment to the injured areas of
446 TSPO expressing microglia cells or modifications in binding site conformation. TSPO
447 ligands are able to modulate the release of pro-inflammatory cytokines like TNF-α and IL-
448 1β from microglia when the activating agent is ATP released from injured neurons (Choi, et
449 al., 2011, Ydens, et al., 2012). Consequently, the earlier increase of TSPO binding in

TREM2$^{-/-}$ mice may be explained as a response to the impaired immune reaction during MPTP-dependent neuronal damage. These results are in line also with data obtained from Bae et al (Bae, et al., 2014) showing that the over-expression of TSPO resulted in a significant *in vitro* reduction in the levels of several pro-inflammatory mediators, including TNF-α, in microglia cells.

Based on this observation, we postulate that in TREM2$^{-/-}$ mice, the increased [^{11}C]PK11195 binding and the down-regulation of pro-inflammatory mediators production might depict an adaptive immune response to neuronal damage. However, as recently observed in an experimental stroke model (Kawabori, et al., 2015, Sieber, et al., 2013), the sub-acute inflammatory reaction developed in absence of TREM2 does not protect brain tissue from an acute neuronal injury.

5. CONCLUSIONS

In conclusion, our results support the prominent role of TREM2 in chronic inflammatory or neurodegenerative CNS disorders, as EAE or AD, rather than in acute neuronal injury. However, also in this case TREM2 might control local inflammation as indicated by its increased expression following a neuronal insult. Indeed, in a neurotoxic model such as that based on MPTP, acute neuronal death is so strong and abrupt that cannot be controlled by TREM2 immunomodulatory activity. The reduced levels of pro-inflammatory cytokines and the earlier increase in TSPO binding observed in TREM2$^{-/-}$ mice, further support the role of this receptor in the regulation of the immune response during acute neuronal injury. As the lack of TREM2 expression does not protect from neuronal loss, the role of neuroinflammation off-switch during acute injury is still questionable.

6. DISCLOSURE STATEMENT

The authors declare that they have not conflict of interest.

7. ACKNOWLEDGMENTS

We thank Susan Gilfillan and Marco Colonna (Department of Pathology and Immunology, Washington University, St. Louis, MO, USA) for providing the TREM2$^{-/-}$ mice. We also thank Valentina Murtaj and Isabella Raccagni for animal tissues preparation and RT-PCR analysis. Fluorescence microscopy was carried out in ALEMBIC, an advanced microscopy laboratory established by the San Raffaele Scientific Institute and the Vita-Salute San Raffaele University.

We kindly thank dr. Letterio S. Politi and Antonella Iadanza for MRI acquisition of MPTP- or PBS-injected TREM2-/- and wt mice.

The research has been partially funded by European Union's Seventh Framework Programme (FP7/2007-2013) under grant agreement n° 278850 (INMiND); Framework Agreement Lombardy Region - National Research Council of Italy (16/7/2012) Project "MbMM - Basic methodologies for innovation in the diagnosis and therapy of multi factorial diseases" (signed 25/7/2013) and the Italian Ministry of Education, University and Research (MIUR) Project: "Identification, validation and commercial development of new diagnostic and prognostic biomarkers for complex trait diseases (IVASCOMAR, Prot. CTN01 00177 165430)".

REFERENCES

Antonini, A., Moresco, R.M., Gobbo, C., De Notaris, R., Panzacchi, A., Barone, P., Bonifati, V., Pezzoli, G., Fazio, F. 2002. Striatal dopaminergic denervation in early and late onset Parkinson's disease assessed by PET and the tracer [11C]FECIT: preliminary findings in one patient with autosomal recessive parkinsonism (Park2). Neurological sciences : official journal of the Italian Neurological Society and of the Italian Society of Clinical Neurophysiology 23 Suppl 2, S51-2. doi:10.1007/s100720200065.

Bae, K.R., Shim, H.J., Balu, D., Kim, S.R., Yu, S.W. 2014. Translocator protein 18 kDa negatively regulates inflammation in microglia. Journal of neuroimmune pharmacology : the official journal of the Society on NeuroImmune Pharmacology 9(3), 424-37. doi:10.1007/s11481-014-9540-6.

Banati, R.B., Newcombe, J., Gunn, R.N., Cagnin, A., Turkheimer, F., Heppner, F., Price, G., Wegner, F., Giovannoni, G., Miller, D.H., Perkin, G.D., Smith, T., Hewson, A.K., Bydder, G., Kreutzberg, G.W., Jones, T., Cuzner, M.L., Myers, R. 2000. The peripheral benzodiazepine binding site in the brain in multiple sclerosis: quantitative in vivo imaging of microglia as a measure of disease activity. Brain 123 (Pt 11), 2321-37.

Bessis, A., Bechade, C., Bernard, D., Roumier, A. 2007. Microglial control of neuronal death and synaptic properties. Glia 55(3), 233-8. doi:10.1002/glia.20459.

Block, M.L., Hong, J.S. 2007. Chronic microglial activation and progressive dopaminergic neurotoxicity. Biochem Soc Trans 35(Pt 5), 1127-32. doi:10.1042/BST0351127.

Bouchon, A., Hernandez-Munain, C., Cella, M., Colonna, M. 2001. A DAP12-mediated pathway regulates expression of CC chemokine receptor 7 and maturation of human dendritic cells. The Journal of experimental medicine 194(8), 1111-22.

Casellas, P., Galiegue, S., Basile, A.S. 2002. Peripheral benzodiazepine receptors and mitochondrial function. Neurochemistry international 40(6), 475-86.

Choi, J., Ifuku, M., Noda, M., Guilarte, T.R. 2011. Translocator protein (18 kDa)/peripheral benzodiazepine receptor specific ligands induce microglia functions consistent with an activated state. Glia 59(2), 219-30. doi:10.1002/glia.21091.

Fenoglio, C., Galimberti, D., Piccio, L., Scalabrini, D., Panina, P., Buonsanti, C., Venturelli, E., Lovati, C., Forloni, G., Mariani, C., Bresolin, N., Scarpini, E. 2007. Absence of TREM2 polymorphisms in patients with Alzheimer's disease and Frontotemporal Lobar Degeneration. Neuroscience letters 411(2), 133-7. doi:10.1016/j.neulet.2006.10.029.

Finelli, D., Rollinson, S., Harris, J., Jones, M., Richardson, A., Gerhard, A., Snowden, J., Mann, D., Pickering-Brown, S. 2015. TREM2 analysis and increased risk of Alzheimer's disease. Neurobiology of aging 36(1), 546 e9-13. doi:10.1016/j.neurobiolaging.2014.08.001.

Halldin, C., Farde, L., Lundkvist, C., Ginovart, N., Nakashima, Y., Karlsson, P., Swahn, C.G. 1996. [11C]beta-CIT-FE, a radioligand for quantitation of the dopamine transporter in the living brain using positron emission tomography. Synapse 22(4), 386-90. doi:10.1002/(SICI)1098-2396(199604)22:4<386::AID-SYN10>3.0.CO;2-W.

Henkel, J.S., Beers, D.R., Zhao, W., Appel, S.H. 2009. Microglia in ALS: the good, the bad, and the resting. Journal of neuroimmune pharmacology : the official journal of the Society on NeuroImmune Pharmacology 4(4), 389-98. doi:10.1007/s11481-009-9171-5.

Hsieh, C.L., Koike, M., Spusta, S.C., Niemi, E.C., Yenari, M., Nakamura, M.C., Seaman, W.E. 2009. A role for TREM2 ligands in the phagocytosis of apoptotic neuronal cells by microglia. Journal of neurochemistry 109(4), 1144-56. doi:10.1111/j.1471-4159.2009.06042.x.

Hynds, D.L., Rangappa, N., Ter Beest, J., Snow, D.M., Rabchevsky, A.G. 2004. Microglia enhance dorsal root ganglion outgrowth in Schwann cell cultures. Glia 46(2), 218-23. doi:10.1002/glia.10353.

Jackson-Lewis, V., Przedborski, S. 2007. Protocol for the MPTP mouse model of Parkinson's disease. Nature protocols 2(1), 141-51. doi:10.1038/nprot.2006.342.

Jay, T.R., Miller, C.M., Cheng, P.J., Graham, L.C., Bemiller, S., Broihier, M.L., Xu, G., Margevicius, D., Karlo, J.C., Sousa, G.L., Cotleur, A.C., Butovsky, O., Bekris, L., Staugaitis, S.M., Leverenz, J.B., Pimplikar, S.W., Landreth, G.E., Howell, G.R., Ransohoff, R.M., Lamb, B.T. 2015. TREM2 deficiency eliminates TREM2+ inflammatory macrophages and ameliorates pathology in Alzheimer's disease mouse models. The Journal of experimental medicine 212(3), 287-95. doi:10.1084/jem.20142322.

Kawabori, M., Kacimi, R., Kauppinen, T., Calosing, C., Kim, J.Y., Hsieh, C.L., Nakamura, M.C., Yenari, M.A. 2015. Triggering receptor expressed on myeloid cells 2 (TREM2) deficiency attenuates phagocytic activities of microglia and exacerbates ischemic damage in experimental stroke. The Journal of neuroscience : the official journal of the Society for Neuroscience 35(8), 3384-96. doi:10.1523/JNEUROSCI.2620-14.2015.

Laakso, A., Bergman, J., Haaparanta, M., Vilkman, H., Solin, O., Hietala, J. 1998. [18F]CFT [(18F)WIN 35,428], a radioligand to study the dopamine transporter with PET: characterization in human subjects. Synapse 28(3), 244-50. doi:10.1002/(SICI)1098-2396(199803)28:3<244::AID-SYN7>3.0.CO;2-A.

Lassmann, H. 2007. New concepts on progressive multiple sclerosis. Current neurology and neuroscience reports 7(3), 239-44.

Long-Smith, C.M., Sullivan, A.M., Nolan, Y.M. 2009. The influence of microglia on the pathogenesis of Parkinson's disease. Progress in neurobiology 89(3), 277-87. doi:10.1016/j.pneurobio.2009.08.001.

Lucignani, G., Gobbo, C., Moresco, R.M., Antonini, A., Panzacchi, A., Bonaldi, L., Carpinelli, A., Caraceni, T., Fazio, F. 2002. The feasibility of statistical parametric mapping for the analysis of positron emission tomography studies using 11C-2-beta-carbomethoxy-3-beta-(4-fluorophenyl)-tropane in patients with movement disorders. Nuclear medicine communications 23(11), 1047-55. doi:10.1097/01.mnm.0000040966.72730.e4.

Minghetti, L., Pocchiari, M. 2007. Cyclooxygenase-2, prostaglandin E2, and microglial activation in prion diseases. International review of neurobiology 82, 265-75. doi:10.1016/S0074-7742(07)82014-9.

Motta, A., Guerra, A.D., Belcari, N., Moehrs, S., Panetta, D., Righi, S., Valentini, D. 2005. Fast 3D-EM reconstruction using Planograms for stationary planar positron emission mammography camera. Computerized medical imaging and graphics : the official journal of the Computerized Medical Imaging Society 29(8), 587-96. doi:10.1016/j.compmedimag.2005.07.002.

Naert, G., Rivest, S. 2011. The role of microglial cell subsets in Alzheimer's disease. Current Alzheimer research 8(2), 151-5.

Napoli, I., Neumann, H. 2010. Protective effects of microglia in multiple sclerosis. Experimental neurology 225(1), 24-8. doi:10.1016/j.expneurol.2009.04.024.

Numasawa, Y., Yamaura, C., Ishihara, S., Shintani, S., Yamazaki, M., Tabunoki, H., Satoh, J.I. 2011. Nasu-Hakola disease with a splicing mutation of TREM2 in a Japanese family. European journal of neurology 18(9), 1179-83. doi:10.1111/j.1468-1331.2010.03311.x.

Painter, M.M., Atagi, Y., Liu, C.C., Rademakers, R., Xu, H., Fryer, J.D., Bu, G. 2015. TREM2 in CNS homeostasis and neurodegenerative disease. Molecular neurodegeneration 10, 43. doi:10.1186/s13024-015-0040-9.

Perry, V.H. 2010. Contribution of systemic inflammation to chronic neurodegeneration. Acta neuropathologica 120(3), 277-86. doi:10.1007/s00401-010-0722-x.

Piccio, L., Buonsanti, C., Cella, M., Tassi, I., Schmidt, R.E., Fenoglio, C., Rinker, J., 2nd, Naismith, R.T., Panina-Bordignon, P., Passini, N., Galimberti, D., Scarpini, E., Colonna, M., Cross, A.H. 2008. Identification of soluble TREM-2 in the cerebrospinal fluid and its association with multiple sclerosis and CNS inflammation. Brain 131(Pt 11), 3081-91. doi:10.1093/brain/awn217.

Piccio, L., Buonsanti, C., Mariani, M., Cella, M., Gilfillan, S., Cross, A.H., Colonna, M., Panina-Bordignon, P. 2007. Blockade of TREM-2 exacerbates experimental autoimmune encephalomyelitis. European journal of immunology 37(5), 1290-301. doi:10.1002/eji.200636837.

Polazzi, E., Monti, B. 2010. Microglia and neuroprotection: from in vitro studies to therapeutic applications. Progress in neurobiology 92(3), 293-315. doi:10.1016/j.pneurobio.2010.06.009.

Poliani, P.L., Wang, Y., Fontana, E., Robinette, M.L., Yamanishi, Y., Gilfillan, S., Colonna, M. 2015. TREM2 sustains microglial expansion during aging and response to demyelination. J Clin Invest 125(5), 2161-70. doi:10.1172/JCI77983.

Przedborski, S., Jackson-Lewis, V., Djaldetti, R., Liberatore, G., Vila, M., Vukosavic, S., Almer, G. 2000. The parkinsonian toxin MPTP: action and mechanism. Restorative neurology and neuroscience 16(2), 135-42.

Rayaprolu, S., Mullen, B., Baker, M., Lynch, T., Finger, E., Seeley, W.W., Hatanpaa, K.J., Lomen-Hoerth, C., Kertesz, A., Bigio, E.H., Lippa, C., Josephs, K.A., Knopman, D.S., White, C.L., 3rd, Caselli, R., Mackenzie, I.R., Miller, B.L., Boczarska-Jedynak, M., Opala, G., Krygowska-Wajs, A., Barcikowska, M., Younkin, S.G., Petersen, R.C., Ertekin-Taner, N., Uitti, R.J., Meschia, J.F., Boylan, K.B., Boeve, B.F., Graff-Radford, N.R., Wszolek, Z.K., Dickson, D.W., Rademakers, R., Ross, O.A. 2013. TREM2 in neurodegeneration: evidence for association of the p.R47H variant with frontotemporal dementia and Parkinson's disease. Molecular neurodegeneration 8, 19. doi:10.1186/1750-1326-8-19.

Sanchez-Guajardo, V., Tentillier, N., Romero-Ramos, M. 2015. The relation between alpha-synuclein and microglia in Parkinson's disease: Recent developments. Neuroscience 302, 47-58. doi:10.1016/j.neuroscience.2015.02.008.

Schmid, C.D., Sautkulis, L.N., Danielson, P.E., Cooper, J., Hasel, K.W., Hilbush, B.S., Sutcliffe, J.G., Carson, M.J. 2002. Heterogeneous expression of the triggering receptor expressed on myeloid cells-2 on adult murine microglia. Journal of neurochemistry 83(6), 1309-20.

Sessa, G., Podini, P., Mariani, M., Meroni, A., Spreafico, R., Sinigaglia, F., Colonna, M., Panina, P., Meldolesi, J. 2004. Distribution and signaling of TREM2/DAP12, the receptor system mutated in human polycystic lipomembraneous osteodysplasia with sclerosing leukoencephalopathy dementia. The European journal of neuroscience 20(10), 2617-28. doi:10.1111/j.1460-9568.2004.03729.x.

Sieber, M.W., Jaenisch, N., Brehm, M., Guenther, M., Linnartz-Gerlach, B., Neumann, H., Witte, O.W., Frahm, C. 2013. Attenuated inflammatory response in triggering

receptor expressed on myeloid cells 2 (TREM2) knock-out mice following stroke. PloS one 8(1), e52982. doi:10.1371/journal.pone.0052982.
Sieger, D., Peri, F. 2013. Animal models for studying microglia: the first, the popular, and the new. Glia 61(1), 3-9. doi:10.1002/glia.22385.
Smeyne, R.J., Jackson-Lewis, V. 2005. The MPTP model of Parkinson's disease. Brain research Molecular brain research 134(1), 57-66. doi:10.1016/j.molbrainres.2004.09.017.
Takahashi, K., Prinz, M., Stagi, M., Chechneva, O., Neumann, H. 2007. TREM2-transduced myeloid precursors mediate nervous tissue debris clearance and facilitate recovery in an animal model of multiple sclerosis. PLoS medicine 4(4), e124. doi:10.1371/journal.pmed.0040124.
Takahashi, K., Rochford, C.D., Neumann, H. 2005. Clearance of apoptotic neurons without inflammation by microglial triggering receptor expressed on myeloid cells-2. The Journal of experimental medicine 201(4), 647-57. doi:10.1084/jem.20041611.
Turkheimer, F.E., Rizzo, G., Bloomfield, P.S., Howes, O., Zanotti-Fregonara, P., Bertoldo, A., Veronese, M. 2015. The methodology of TSPO imaging with positron emission tomography. Biochem Soc Trans 43(4), 586-92. doi:10.1042/BST20150058.
Turnbull, I.R., Gilfillan, S., Cella, M., Aoshi, T., Miller, M., Piccio, L., Hernandez, M., Colonna, M. 2006. Cutting edge: TREM-2 attenuates macrophage activation. Journal of immunology 177(6), 3520-4.
Van Der Putten, C., Kuipers, H.F., Zuiderwijk-Sick, E.A., Van Straalen, L., Kondova, I., Van Den Elsen, P.J., Bajramovic, J.J. 2012. Statins amplify TLR-induced responses in microglia via inhibition of cholesterol biosynthesis. Glia 60(1), 43-52. doi:10.1002/glia.21245.
Veiga, S., Carrero, P., Pernia, O., Azcoitia, I., Garcia-Segura, L.M. 2007. Translocator protein 18 kDa is involved in the regulation of reactive gliosis. Glia 55(14), 1426-36. doi:10.1002/glia.20558.
Venkatesan, C., Chrzaszcz, M., Choi, N., Wainwright, M.S. 2010. Chronic upregulation of activated microglia immunoreactive for galectin-3/Mac-2 and nerve growth factor following diffuse axonal injury. Journal of neuroinflammation 7, 32. doi:10.1186/1742-2094-7-32.
Wang, Y., Cella, M., Mallinson, K., Ulrich, J.D., Young, K.L., Robinette, M.L., Gilfillan, S., Krishnan, G.M., Sudhakar, S., Zinselmeyer, B.H., Holtzman, D.M., Cirrito, J.R., Colonna, M. 2015. TREM2 lipid sensing sustains the microglial response in an Alzheimer's disease model. Cell 160(6), 1061-71. doi:10.1016/j.cell.2015.01.049.
Wang, Y., Ulland, T.K., Ulrich, J.D., Song, W., Tzaferis, J.A., Hole, J.T., Yuan, P., Mahan, T.E., Shi, Y., Gilfillan, S., Cella, M., Grutzendler, J., DeMattos, R.B., Cirrito, J.R., Holtzman, D.M., Colonna, M. 2016. TREM2-mediated early microglial response limits diffusion and toxicity of amyloid plaques. The Journal of experimental medicine 213(5), 667-75. doi:10.1084/jem.20151948.
Wes, P.D., Sayed, F.A., Bard, F., Gan, L. 2016. Targeting microglia for the treatment of Alzheimer's Disease. Glia 64(10), 1710-32. doi:10.1002/glia.22988.
Winkeler, A., Boisgard, R., Awde, A.R., Dubois, A., Theze, B., Zheng, J., Ciobanu, L., Dolle, F., Viel, T., Jacobs, A.H., Tavitian, B. 2012. The translocator protein ligand [(1)(8)F]DPA-714 images glioma and activated microglia in vivo. European journal of nuclear medicine and molecular imaging 39(5), 811-23. doi:10.1007/s00259-011-2041-4.
Yadav, A., Collman, R.G. 2009. CNS inflammation and macrophage/microglial biology associated with HIV-1 infection. Journal of neuroimmune pharmacology : the

official journal of the Society on NeuroImmune Pharmacology 4(4), 430-47. doi:10.1007/s11481-009-9174-2.

Ydens, E., Cauwels, A., Asselbergh, B., Goethals, S., Peeraer, L., Lornet, G., Almeida-Souza, L., Van Ginderachter, J.A., Timmerman, V., Janssens, S. 2012. Acute injury in the peripheral nervous system triggers an alternative macrophage response. Journal of neuroinflammation 9, 176. doi:10.1186/1742-2094-9-176.

FIGURE LEGENDS

Figure 1. **TREM2 regional brain expression in C57BL/6 and MPTP treated mice.** RT-PCR analysis of TREM2 expression in the different brain areas of mice treated with MPTP at day 1, 2 and 7 after intoxication compared to controls (PBS). TREM2 mRNA expression of 7 mice per time point is reported. All the values were normalized to mouse β-actin and expressed as fold change (F.C.). ONE-way ANOVA, Dunnett's correction; * $p<0,05$; ** $p<0,01$ compared to PBS condition.

Figure 2. Nuroinflammation and microglia activation after MPTP treatment. 5 to 7 mice per group were injected with PBS or MPTP and were sacrificed 1, 2 and 7 days after toxin injection. Striatum and SN, were dissected and processed for RT-PCR analysis or immunofluorescence staining. (A) RT-PCR analysis of Gal-3 mRNA expression in the striatum and SN of MPTP-treated mice at days 1, 2 and 7 or PBS injected animals. ONE-way ANOVA, Dunnett's correction; **$p<0,01$; ***$p<0,001$, compared to PBS condition. (B) Immunofluorescence staining of Iba-1 (a) and GFAP (b) positive cells in striatum of

PBS and MPTP injected animals after 1, 2 and 7 days. Bar: 200µm; insets: 2x magnification. (C) Percentage of Iba-1 and GFAP positive cells in striatum of PBS and MPTP injected animals after 1, 2 and 7 days. Student's t test, *p<0,05, **p<0,01, ***p<0,001, compared to the corresponding baseline (PBS) condition.

Figure 3. Microglia activation and expression of pro-inflammatory and phagocytosis markers after MPTP treatment.

5 to 7 mice per group were injected with PBS or MPTP and were sacrificed 1, 2 and 7 days after toxin treatment. Striatum and SN were dissected and processed for [^{11}C]PK11195 uptake measure or RT-PCR analysis of inflammation markers. (A) [^{11}C]PK11195 uptake in the striatum and SN of PBS injected and MPTP treated mice at day 1, 2 and 7. Data are expressed as percentage of the injected dose per gram of tissue (%ID/g); Student's t test; **p<0,01, compared to PBS. (B) RT-PCR analysis of TSPO mRNA in the striatum of PBS injected or MPTP treated mice at day 1, 2 and 7. Student's t test; ***p<0,001. (C) RT-PCR analysis of TNF-α mRNA expression in the striatum (left) and SN (Venkatesan, et al.) of PBS injected or MPTP treated mice at day 1, 2 and 7. ONE-way ANOVA, Dunnett's correction; **p< 0,01, ***p< 0,001. (D) RT-PCR analysis of IL-1β and IL-4 mRNA in the striatum of PBS injected or MPTP treated mice at day 1, 2 and 7. Student's t test; *p<0,5 and ***p<0,001. IL-4 expression increased at 7 days post-MPTP; Student's test; **p<0,01.

Figure 4. Microglia activation in TREM2$^{-/-}$ and wt mice at day 1 after MPTP injection.

Three mice per group were injected with PBS or MPTP and sacrificed 1 day after toxin treatment. Striatum was dissected and processed for immunofluorescence staining, [^{11}C]PK11195 uptake measure or TSPO RT-PCR analysis. (A) Percentage of Iba-1 and GFAP positive cells in striatum of wt and TREM2$^{-/-}$ mice after PBS or MPTP injection (1 day); Student's t test, *p<0,05, **p<0,01. (B) Immunofluorescence staining of Iba-1 (a) and GFAP (b) positive cells in striatum of PBS and MPTP injected animals after 1 day. Bar: 400

747 µm. (C) [^{11}C]PK11195 uptake in striatum and SN of wt and TREM2$^{-/-}$ mice, at day 1 after
748 PBS or MPTP treatment. [^{11}C]PK11195 uptake was increased in TREM2$^{-/-}$ MPTP-treated
749 mice versus both TREM2$^{-/-}$-untreated and wt MPTP-treated mice in striatum and SN;
750 Student's t test; *p<0,05, **p<0,01 compared to TREM2$^{-/-}$ PBS and $^{\#}$p<0,05 between wt
751 MPTP and TREM2$^{-/-}$ MPTP. (D) RT-PCR analysis of TSPO mRNA in the striatum of PBS
752 injected or MPTP treated mice at day 1. Student's t test.

753 **Figure 5. Expression of pro-inflammatory and phagocytosis markers in TREM2$^{-/-}$ and**
754 **wt mice at day 1 after MPTP injection.**

755 Three or 6-7 mice per group were injected with PBS or MPTP and sacrificed 1 day after
756 toxin treatment. Striatum and substantia nigra were dissected and processed for RT-PCR
757 analysis inflammation markers. (A) Gal-3 and TNF-α mRNA expression was measured by
758 RT-PCR analysis in PBS or MPTP injected wild type (wt) and TREM2$^{-/-}$ mice (6-7 mice per
759 group) at 1 day after MPTP. All values were normalized to β-actin mRNA expression.
760 Student's t test, Mann Whitney's correction; ***p<0.001. (B) RT-PCR analysis of IL-1β and
761 IL-4 mRNA in the striatum of PBS injected or MPTP treated mice (3 mice per group) at day
762 1. Student's t test; *p<0,05 and ***p<0,001. IL-4 expression was at baseline lower in
763 TREM2$^{-/-}$ compared to wt; Student's test; *p<0,05.

764 **Figure 6: DAT radioligand [^{11}C]FECIT uptake in wild type and TREM2$^{-/-}$ mice.** Four to
765 twenty-one mice per group were injected with PBS or MPTP and sacrificed 1, 2 and 7 days
766 after toxin treatment for *ex vivo* and *in vivo* evaluation of dopamine transporter (DAT). (A)
767 *Ex vivo* [^{11}C]FECIT binding in striatum of PBS (four mice) and MPTP-injected C57BL/6
768 mice (five mice per time point) at 1, 2 and 7 days after treatment. Data are expressed as ratio
769 between radioactivity concentration in striatum and cerebellum. Student's t test; **p<0,01
770 and ***p<0,001 compared to PBS. (B) Summary of [^{11}C]FECIT binding values of wild type
771 (n= 16) and TREM2$^{-/-}$ mice (n= 21). [^{11}C]FECIT uptake is represented as the ratio between

772 the uptake level in the striatum and the cerebellum of PBS or MPTP injected wild type
773 (black bars) and TREM2$^{-/-}$ (gray bars) mice, 7 days post-treatment. Student's t test;
774 **p<0,01 compared to the corresponding PBS. (C) *In vivo* brain imaging of [^{11}C]FECIT
775 uptake of PBS or MPTP injected wt (I and II, respectively) and TREM2$^{-/-}$ (III and IV,
776 respectively) mice. Images represent the coronal view taken at the level of striatum (arrows).
777 Correspondent MRI images and superimposed striatal ROIs are presented in panel V (top,
778 coronal and bottom, axial).
779
780
781
782

*Verification

Verification statement of authors of the manuscript NBA-14-844 entitled "Early up-regulation of 18 kDa Translocator Protein in response to acute neurodegenerative damage in TREM2 deficient mice"

1. The authors of this manuscript declare that:
   (a) they have not conflict of interest
   (b) and also their institution have not conflict of interest
   (c) or financial interest in this work.
2. The research of this manuscript was supported by the following grants:
   - European Union's Seventh Framework Programme (FP7/2007-2013) under grant agreement n° 278850 (INMiND);
   - Framework Agreement Lombardy Region - National Research Council of Italy (16/7/2012) Project "MbMM - Basic methodologies for innovation in the diagnosis and therapy of multi factorial diseases" (signed 25/7/2013);
   - the Italian Ministry of Education, University and Research (MIUR) Project: "Identification, validation and commercial development of new diagnostic and prognostic biomarkers for complex trait diseases (IVASCOMAR, Prot. CTN01 00177 165430)".
3. The data contained in this manuscript have not been previously published or submitted or under consideration to other Journals.
4. Animal experiments were carried out in compliance with the institutional guidelines for the care and use of experimental animals (IACUC), which have been notified to the Italian Ministry of Health and approved by the Ethics Committee of the San Raffaele Scientific Institute (Protocols n. 722 of 29/02/2016 and n.723 12/01/2016).
5. All authors have reviewed the contents of the manuscript being submitted, approved its contents and validated the accuracy of the data.

Milan, the 8th November, 2016

Sincerely,

Rosa Maria Moresco

Figure 1

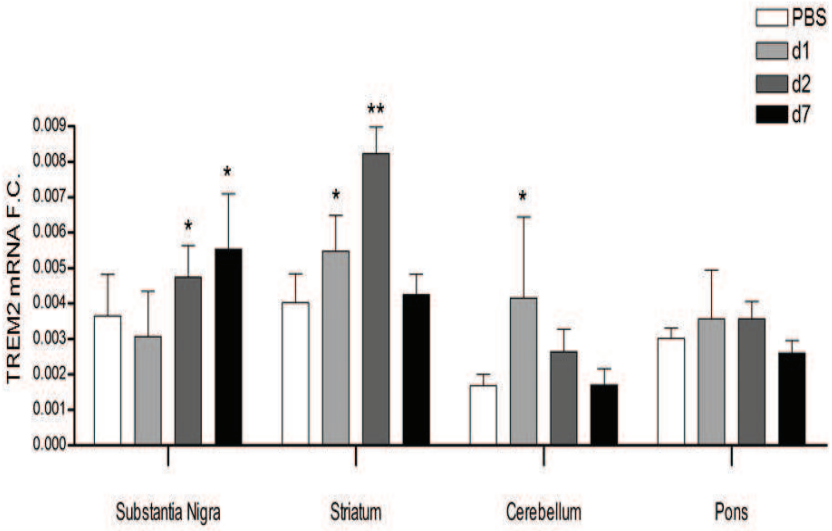
PBS
d1
d2
d7
TREM2 mRNA F.C.
0.009
0.008
0.007
0.006
0.005
0.004
0.003
0.002
0.001
0.000
*
*
*
**
*
Substantia Nigra
Striatum
Cerebellum
Pons

Figure 2

Figure 2

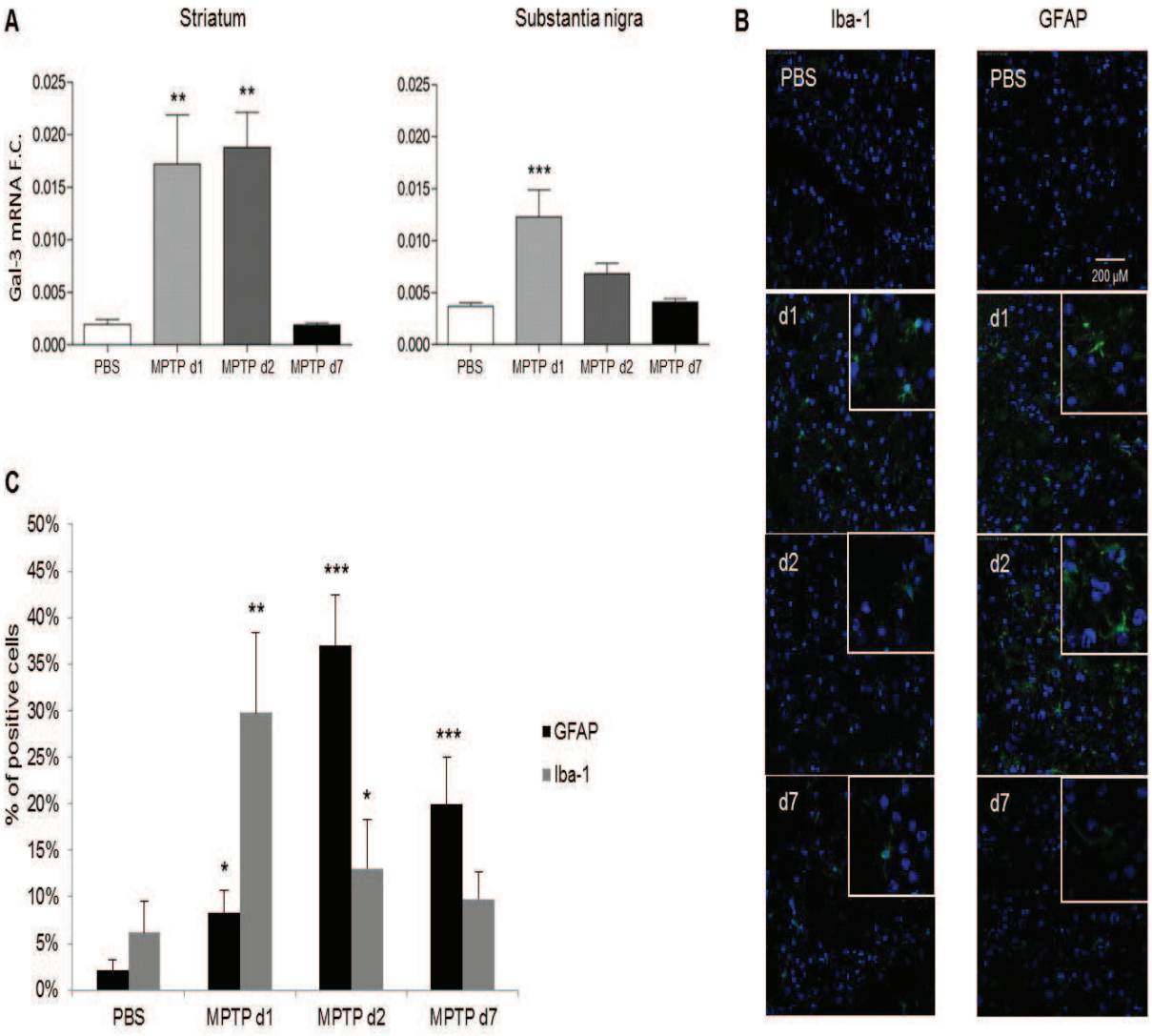

Figure 3

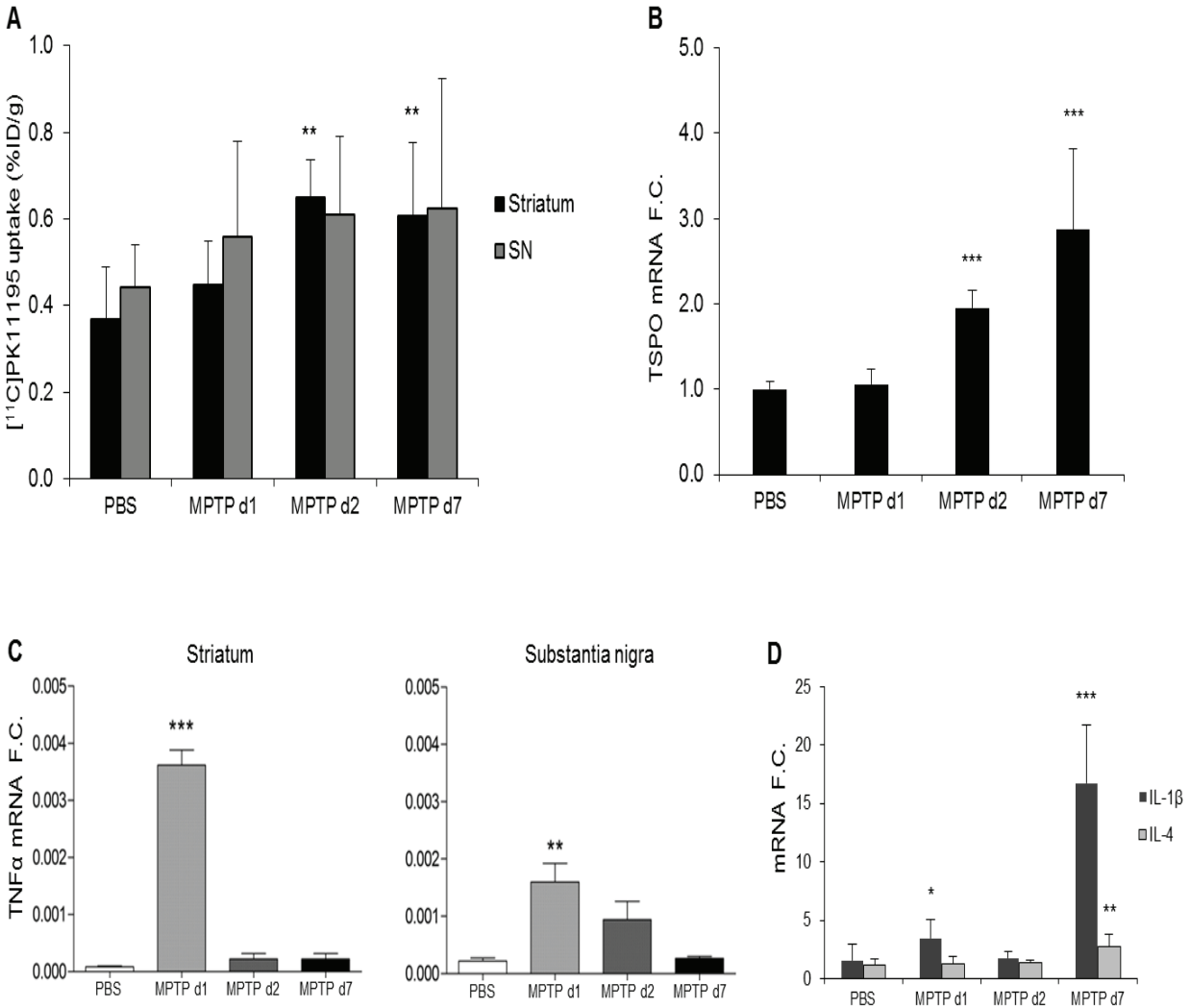
A
[11C]PK11195 uptake (%ID/g)
1.0
0.8
0.6
0.4
0.2
0.0
**
**
Striatum
SN
PBS
MPTP d1
MPTP d2
MPTP d7
B
TSPO mRNA F.C.
5.0
4.0
3.0
2.0
1.0
0.0
***
***
PBS
MPTP d1
MPTP d2
MPTP d7
C
Striatum
TNFα mRNA F.C.
0.005
0.004
0.003
0.002
0.001
0.000
***
PBS
MPTP d1
MPTP d2
MPTP d7
Substantia nigra
0.005
0.004
0.003
0.002
0.001
0.000
**
PBS
MPTP d1
MPTP d2
MPTP d7
D
mRNA F.C.
25
20
15
10
5
0
***
*
**
IL-1β
IL-4
PBS
MPTP d1
MPTP d2
MPTP d7

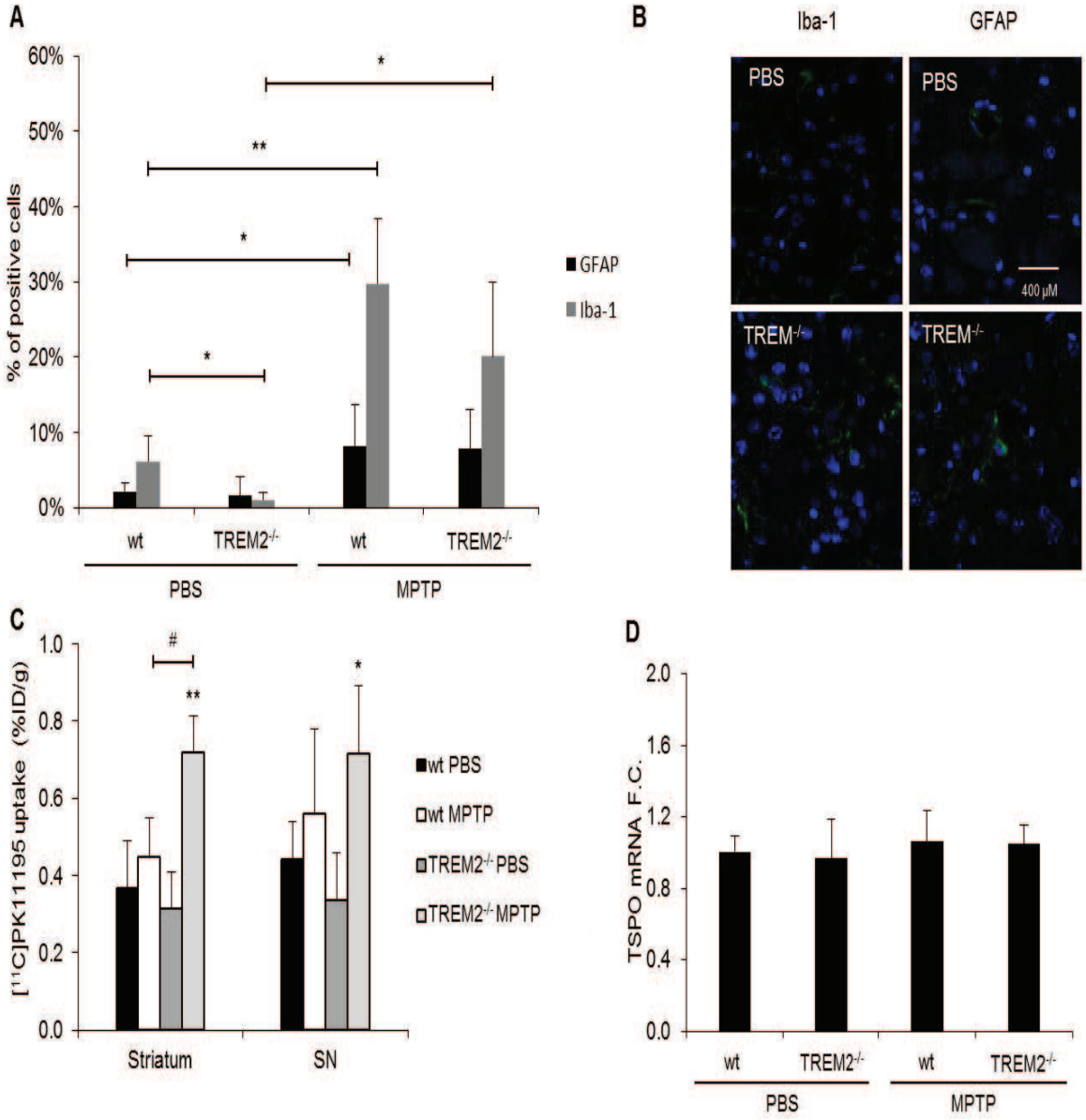
A
60%
50%
40%
30%
20%
10%
0%
% of positive cells
*
**
*
*
GFAP
Iba-1
wt
TREM2-/-
wt
TREM2-/-
PBS
MPTP
B
Iba-1
GFAP
PBS
PBS
400 µM
TREM-/-
TREM-/-
C
1.0
0.8
0.6
0.4
0.2
0.0
[11C]PK11195 uptake (%ID/g)
#
**
*
wt PBS
wt MPTP
TREM2-/- PBS
TREM2-/- MPTP
Striatum
SN
D
2.0
1.6
1.2
0.8
0.4
0.0
TSPO mRNA F.C.
wt
TREM2-/-
wt
TREM2-/-
PBS
MPTP

Figure 4

Figure 5

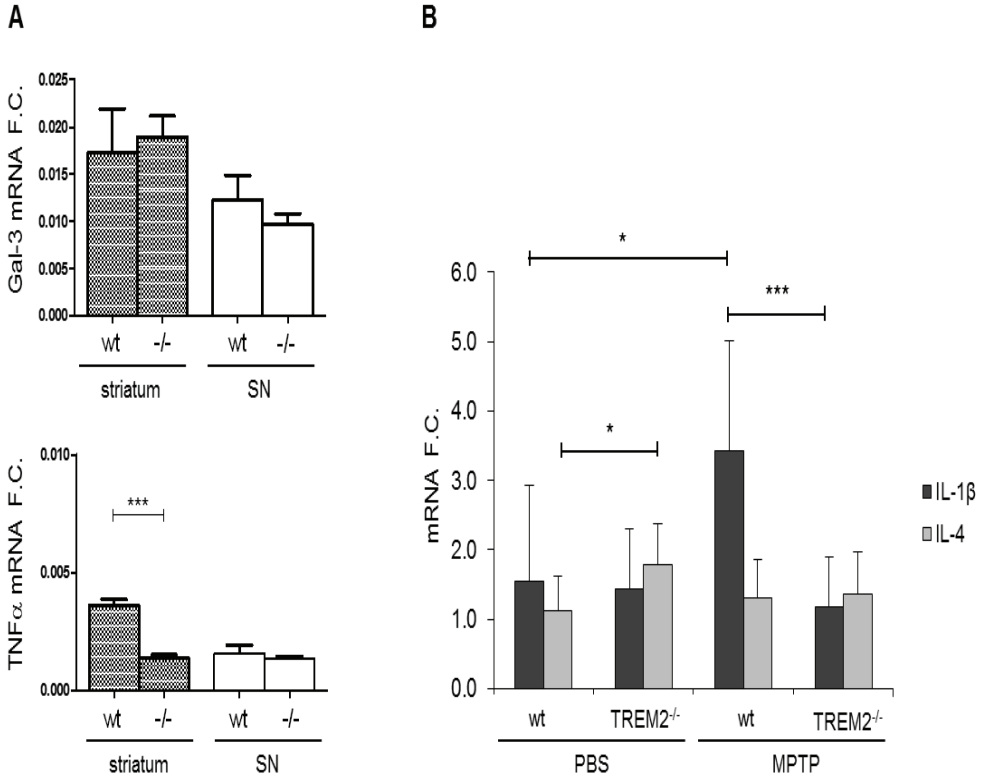
A
Gal-3 mRNA F.C.
0.025
0.020
0.015
0.010
0.005
0.000
wt
-/-
wt
-/-
striatum
SN
TNFα mRNA F.C.
0.010
0.005
0.000
***
wt
-/-
wt
-/-
striatum
SN
B
mRNA F.C.
6.0
5.0
4.0
3.0
2.0
1.0
0.0
*
*
***
IL-1β
IL-4
wt
TREM2-/-
wt
TREM2-/-
PBS
MPTP

Figure 6

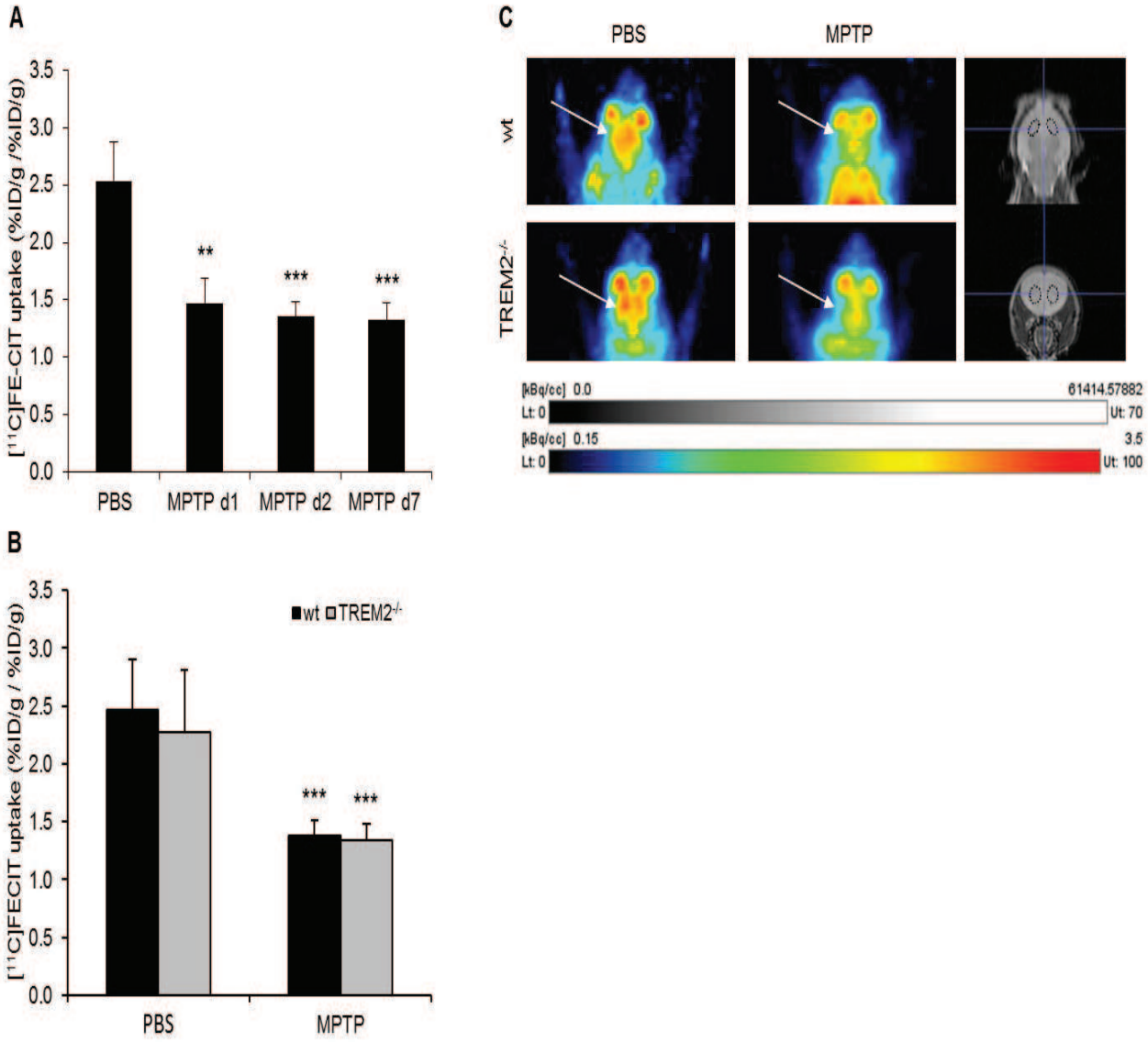
A
[11C]FE-CIT uptake (%ID/g /%ID/g)
3.5
3.0
2.5
2.0
1.5
1.0
0.5
0.0
**
***
***
PBS
MPTP d1
MPTP d2
MPTP d7
B
[11C]FECIT uptake (%ID/g / %ID/g)
wt
TREM2-/-
***
***
PBS
MPTP
C
PBS
MPTP
wt
TREM2-/-
[kBq/cc] 0.0
61414.57882
Lt: 0
Ut: 70
[kBq/cc] 0.15
3.5
Lt: 0
Ut: 100